JOURNAL OF THERMOPHYSICS AND HEAT TRANSFER
Vol. 20, No. 1, January–March 2006

Approximate Thermal Emission Models of a Two-Dimensional Graded Index Semitransparent Medium

Yong Huang* and Xin-Gang Liang†
Tsinghua University, 100084 Beijing, People's Republic of China

This study develops numerical models for thermal emission in a two-dimensional semitransparent graded-index medium. Two piecewise continuous refractive index models, the bar model and the slab model, are presented. The formal is a combination of rectangular bars each having its own unique refractive index. The latter is a combination of slabs, each of which has a linear refractive index distribution. Two interface hypotheses are discussed: the reflection/refraction hypothesis and the refraction/total reflection hypothesis. The backward ray tracing method and the backward Monte Carlo method are employed for calculation. The apparent directional emissivity of a semitransparent medium with linear and nonlinear refractive index distributions is calculated. The results show that piecewise continuous refractive index can be used for modeling semitransparent media with continuously variable refractive index. Emission from the medium is complex and quite different from a medium with a constant refractive index, when the absorption coefficient is small and/or the refractive index varies greatly in the medium. The refractive/totally reflective inner interface in the bar model gives a more precise emission distribution and can be extended to simulate emission from a medium with a complex three-dimensional refractive index distribution.

Nomenclature

a	=	value of $\Delta n_x/DX$ and $\Delta n_y/DY$ when they are equal
DX, DY	=	lengths of the medium in x and y direction, respectively, m
I	=	radiative intensity, W/m$^2 \cdot$ sr
i, j	=	bar or slab identifier
l	=	path length of a ray transferred in the medium, m
N	=	number of Monte Carlo bundles
NX, NY	=	numbers of the discrete pieces in x and y directions, respectively
n	=	refractive index
n_0	=	refractive index of the medium at position $(x, y) = (0, 0)$
$n(i, j)$	=	refractive index of a discrete bar
$n(x, j)$	=	refractive index distribution in a discrete slab
$n(x, y)$	=	refractive index distribution in a two-dimensional medium
s	=	length of curved path, m
T	=	temperature, K
x, y	=	Cartesian coordinates, m
$y(x)$	=	ray equation
$y'(x)$	=	derivative of $y(x)$
α	=	rotation angle, deg
Δn_x, Δn_y	=	refractive index difference in x and y directions, respectively
δ	=	relative error
δ_x, δ_y	=	lengths of the semitransparent pieces in x and y directions, respectively, m
ε	=	apparent directional emissivity
$\varepsilon_{\text{approximate model}}$	=	apparent directional emissivity calculated by the bar or slab model
$\varepsilon_{\text{real model}}$	=	apparent directional emissivity calculated by the real model
ζ	=	incident angle, deg
θ	=	angle between ray's direction and Y axis or refractive angle, deg
κ	=	absorption coefficient, 1/m
ξ, η	=	Cartesian coordinates, m
ρ	=	reflectivity calculated by Fresnel's law
$\rho_\perp$	=	perpendicular reflectivity
φ	=	emission angle, deg

Subscripts and Superscripts

b	=	black body
n	=	ray identifier
t	=	total reflection
1	=	initial position of a ray in a piece of slab
2	=	terminal position of a ray in a piece of slab
$\rightarrow$	=	direction vector

I. Introduction

THE effect of refractive index on radiative transfer in a semitransparent medium layer or composite has been investigated in the last decade.[1–4] Recently, radiative transfer in graded-index (GRIN) media has become attractive[5–10] to researchers. This research is based on the following two facts.

The first is that graded-index effects accompanied by a thermal process broadly exist in nature. For example, when we are burning a piece of paper, we can see that an object on the other side of the flame appears to be distorted to the naked eye. The reason is that the air's refractive index is changed nonuniformly when it is heated by the flame. Also, when a high-energy laser beam propagates in the air, a phenomenon named thermal blooming occurs. The air is heated by the laser, and its refractive index is changed so that the laser beam departs from its original trajectory. Thermal blooming is a fatal problem in the application of high-energy lasers.[11] Refractive index of some semitransparent solid materials also changes with temperature. This will reduce the precision of optical instruments, such as space telescopes and space cameras, which are in complex and variable thermal surroundings.[12,13] Graded-index effects accompanied by thermal processes can cause damage to some engineering processes. Sometimes this phenomenon is inevitable.

Received 24 April 2004; revision received 26 March 2005; accepted for publication 18 April 2005.

*Postdoctor, Department of Engineering Mechanics; The Key Laboratory of Enhanced Heat Transfer and Energy Conservation at Tsinghua University, Ministry of Education; huangy_zl@263.net.

†Professor, Department of Engineering Mechanics; The Key Laboratory of Enhanced Heat Transfer and Energy Conservation at Tsinghua University, Ministry of Education; liangxg@tsinghua.edu.cn.

It is necessary to investigate its effects so that they can be evaluated correctly and unexpected side effects can be avoided.

The second fact is that man-made graded-index materials have promising applications today. They are superior to the constant refractive-index materials in building lighter, smaller, and higher-quality optical systems. GRIN materials are now used in optical fibers, endoscopes, minicameras, and other fields.[14] They can improve the absorption characteristics of solar-energy systems. An example is a solar selective coating,[15,16] which has been recently manufactured using GRIN materials with improved techniques. Like conventional optical materials, heat-transfer processes are considered in the manufacture and application of GRIN materials. The thermal analysis and the thermal design of GRIN materials are not only important to the optical instruments, which are placed in complex thermal surroundings, but are also helpful in the manufacture of GRIN materials.

The study of thermal radiative transfer within GRIN materials is somewhat different from that for GRIN optics and is far from enough. In the study of GRIN optics, only the curved trajectory along the optical axis needs to be considered, whereas thermal emission and absorption in all directions need to be considered in the study of thermal radiative transfer within GRIN materials. On this topic, most researchers have discussed one-dimensional problems,[5,7–10,17] but few have explored multidimensional problems.[6,18] The solution methods applied to multidimensional problems for uniform refractive index media cannot be easily applied to arbitrary refractive index media. The numerical techniques for solving such problems have not been set up yet. In the early 1990s, Siegel and Spuckler[1] developed a model of a one-dimensional composite medium with several sublayers. Each sublayer was treated as a slab with uniform index bounded by diffuse surfaces. The authors expressed the idea that increasing the number of sublayers could approach the radiative behavior of the medium with a continuously varying refractive index. This idea was used to determine the radiative transfer within a one-dimensional graded-index semitransparent medium, and the results fit the exact solutions well.[9] Whether this idea could be applicable to multidimensional problems is unknown. If the answer is positive, what is the strategy for numerical simulation?

This paper focuses on two aspects. The first discusses the models that can best approximate thermal emission in a two-dimensional graded-index semitransparent medium. The second is the study of thermal emission in a two-dimensional graded-index semitransparent medium.

II. Physical Model and Solution

A. Physical Model

Figures 1a and 1b are illustrations of two approximate composite models for a semitransparent continuous refractive-index medium with a cross-sectional area of $DX \times DY$. The first is a bar model, consisting of $NX \times NY$ bars, each of whose cross-sectional areas is $\delta x \times \delta y$. Each bar has a constant refractive index, $n(i, j)(i = 1, 2, 3, \ldots, NX;\ j = 1, 2, 3, \ldots, NY)$, and a constant absorptive coefficient.

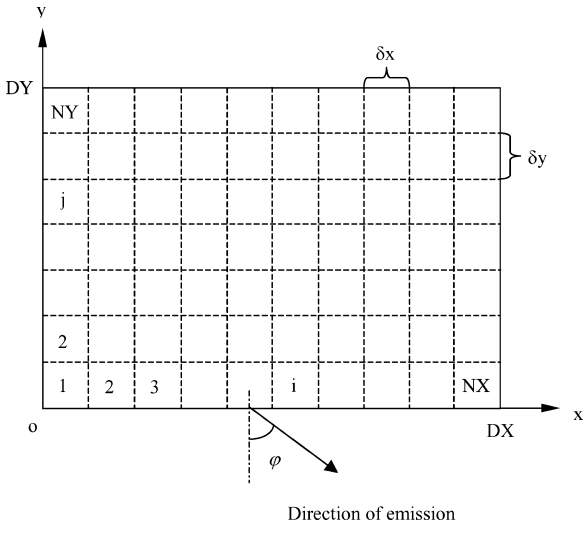

Fig. 1a Composite configuration 1—bar model.

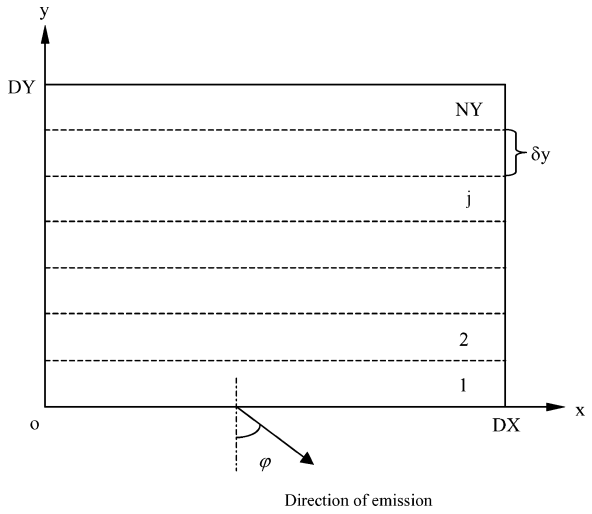

Fig. 1b Composite configuration 2—slab model.

The second is a slab model, composed of NY slabs, each of whose cross-sectional areas is $DX \times \delta y$. In this paper, we discuss two different cases of refractive index variation, one with linear variation in both the x and y directions and one with a linear variation in the x direction and nonlinear variation in the y direction. For instance, in the slab model each slab has a linear refractive index distribution as

$$n(x, j) = n(0, j) + \frac{[n(DX, J) - n(0, j)]x}{DX} \quad (j = 1, 2, 3, \ldots, NY) \quad (1)$$

The surfaces between the bars and the surroundings are assumed to be semitransparent and specularly reflective. Two types of inner interface hypotheses between bars are investigated, refraction/total reflection and reflection/refraction. The first only considers refraction or total reflection. It ignores reflection except for total reflection at the inner interface. The second hypothesis considers reflection and refraction that strictly obey the classical Snell's law and Fresnel's law. The first hypothesis is maybe better than the second in approaching radiative transfer in a two-dimensional GRIN medium because only total reflection happens in a GRIN medium.

This paper considers the emission from the bottom of a semitransparent medium in the *xoy* plane, and the direction of this emission is shown in Figs. 1a and 1b.

B. Solution Method

Under the condition of inner interface hypothesis 1 (refraction/total reflection), the backward ray tracing method can be employed to calculate thermal emission with higher precision and less CPU time. Under the condition of inner interface hypothesis 2 (reflection/refraction), the light will split into a reflecting part and a refracting part. The ray splitting and tracing method[9,10] or the backward Monte Carlo (BMC) method[19] can be employed for the calculation. This paper uses BMC to solve the problem. The computational algorithm for the solution of apparent directional emission by BMC can be summarized as follows[19]:

Step 1: Select the incident angle (emitting angle) φ and the number of rays N in this direction;

Step 2: Calculate the reflectivity of the emitting surface according to the incident angle and the refractive angle of the ray trajectory. Whether each specific ray is reflected or not is controlled by the reflectivity.

Step 3: Trace the ray, which is not reflected at the emitting surface. The distance that the ray could go before it is absorbed is determined

by a random number uniformly distributed between (0, 1). The distance can be derived by a random number according to the Bouguer law and MC theory. If the distance is great enough that the ray can reach the adjacent inner interface, then whether the ray is reflected or refracted is determined by the interface reflectivity. The ray is traced until it is absorbed or it goes out of the medium;

Step 4: Calculate the ray intensity I_n by the integral along the trajectory of the ray[19]

$$I_n = \int_o^l \kappa I_b \, \mathrm{d}l' \tag{2}$$

where l is the path length of the ray transferred in the medium. If the medium is isothermal, I_n can be simplified into

$$I_n = \kappa I_b l \tag{3}$$

where I_b is the blackbody radiation intensity;

Step 5: Average the thermal emission intensity I in the direction φ as

$$I = \frac{1}{N} \sum_{n=1}^{N} I_n \tag{4}$$

C. Curved Ray Tracing

For the slab model, the curved route of a ray is governed by the Fermat principle.[14] Five typical paths in a sublayer for $n(DX, j) > n(0, j)$ are shown in Fig. 2a.

The ray equation in a linearly varying refractive index medium is[5,10]

$$y(x) = n(x_1, j) \sin\theta_1 \int_{x_1}^{x} \frac{\mathrm{d}x}{\sqrt{n^2(x, j) - n^2(x_1, j)\sin^2\theta_1}} + y_1$$

$$= \frac{n(x_1, j)\sin\theta_1 DX}{n(DX, j) - n(0, j)} \int_{x_1}^{x} \frac{\mathrm{d}n(x, j)}{\sqrt{n^2(x, j) - n^2(x_1, j)\sin^2\theta_1}} + y_1 \tag{5}$$

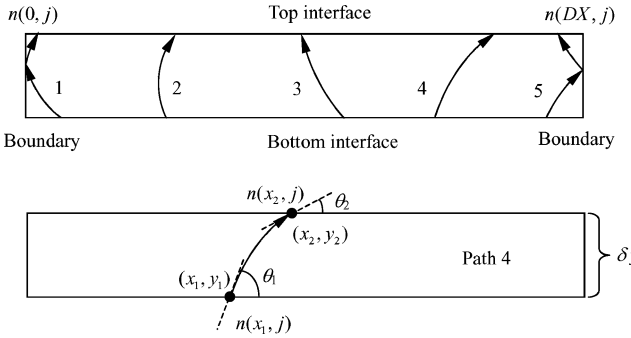

Fig. 2a Five typical paths of ray tracing, $n\,(DX, j) > n\,(0, j)$.

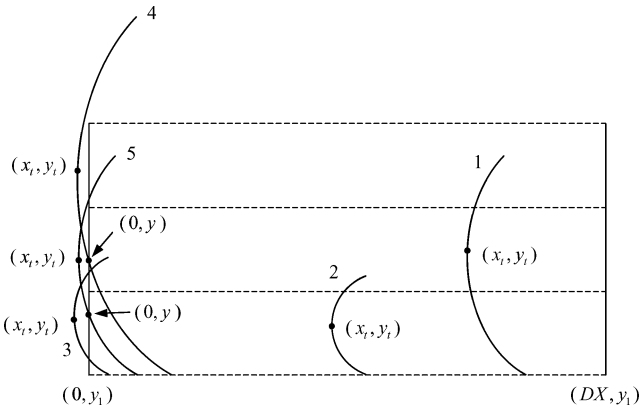

Fig. 2b Five cases of total reflection.

The initial position (x_1, y_1) of a ray is at the bottom interface of a slab, and it will be illustrated through the following cases how the ray reaches its destination (x_2, y_2) at the top interface of the slab.

For those cases matching $\boldsymbol{x}_1 \geq 0$ and $y_2 = y_1 + \delta y$, if x_2 is less than DX, the ray will reach the top interface directly (see path 4 in Fig. 2a); otherwise, it will be reflected by the boundary before it can reach the top interface (see path 5 in Fig. 2a).

When $\boldsymbol{x}_1 < 0$, the total reflection point $((x_t, y_t)$ should be calculated first, although this point might be outside the medium, and then total reflection does not happen. In that case, a virtual point that has the characteristics of total reflection can be designated. If $x_t > 0$ and $y_t - y_1 > \delta y$ (case 1 in Fig. 2b), the ray will reach the top interface directly (path 3 in Fig. 2a). If $x_t > 0$ and $y_t - y_1 \leq \delta y$ (case 2 in Fig. 2b), the ray will reach the top interface after total reflection in the sublayer (path 2 in Fig. 2a). If $x_t \leq 0$ and $y_t - y_1 < \delta y$ (case 3 in Fig. 2b), the ray will be reflected at the left boundary before it can reach the top interface (path 1 in Fig. 2a). If $x_t \leq 0$ and $y_t - y_1 > \delta y$ and if $y - y_1 > \delta y$ for $x = 0$ (case 4 in Fig. 2b), then the ray will reach the top interface directly; or else (case 5 in Fig. 2b) the ray will reflect from the left boundary before it reaches the other interface (path 1 in Fig. 2a).

Following is an example of the calculation of path 4. The ray will reach the sublayer's top interface directly, for which $\boldsymbol{x}_1 \geq 0$ in Fig. 2a. From Eq. (5), for $\boldsymbol{x}_1 \geq 0$ and $y_2 - y_1 = \delta y$, we have

$$\frac{\delta y[n(DX, j) - n(0, j)]}{n(x_1, j)\sin\theta_1 DX} = \int_{x_1}^{x_2} \frac{\mathrm{d}n(x, j)}{\sqrt{n^2(x, j) - n^2(x_1, j)\sin^2\theta_1}}$$

$$= \ell_n \left| \frac{n(x_2, j) + \sqrt{n^2(x_2, j) - n^2(x_1, j)\sin^2\theta_1}}{n(x_1, j) + \sqrt{n^2(x_1, j) - n^2(x_1, j)\sin^2\theta_1}} \right| \tag{6}$$

Hence, x_2 can be deduced as

$$x_2 = \left(\left\{ \left[(1 + \cos\theta_1)^2 \exp \frac{2\delta y n(DX, j) - n(0, j)}{DX n(x_1, j)\sin\theta_1} + \sin^2\theta_1 \right] \Big/ 2(1 + \cos\theta_1) \exp \frac{\delta y n(DX, j) - n(0, j)}{DX n(x_1, j)\sin\theta_1} \right\} n(x_1, j) - n(0, j) \right) \times \frac{DX}{n(DX, j) - n(0, j)} \tag{7}$$

Then, the length s of this curved path and the direction of the light θ_2 at the new position can be calculated as

$$s = \int_{x_1}^{x_2} \sqrt{1 + y'^2(x)}\, \mathrm{d}x = \int_{x_1}^{x_2} \frac{n(x, j)}{\sqrt{n^2(x, j) - n^2(x_1, j)\sin^2\theta_1}} \mathrm{d}x$$

$$= \frac{DX}{n(DX, j) - n(0, j)} \times \left[\sqrt{n^2(x_2, j) - n^2(x_1, j)\sin^2\theta_1} - n(x_1, j)\cos\theta_1 \right] \tag{8}$$

$$\theta_2 = \arcsin\left[\frac{n(x_1, j)\sin\theta_1}{n(x_2, j)} \right] \tag{9}$$

$$\boldsymbol{x}_2 = \cos\theta_2 \qquad \boldsymbol{y}_2 = \sin\theta_2 \tag{10}$$

III. Results and Discussion

In this section we investigate the thermal emission in a two-dimensional GRIN medium using the bar model and the slab model and compare the results with those from a continuous refractive-index medium. The study focuses on thermal emission at the bottom $(y = 0)$ of the composite, which could be isothermal or nonisothermal. The apparent directional emissivity is defined as the ratio of the apparent radiative intensity to the blackbody intensity at the maximum temperature inside the medium.

A. Comparison of Piecewise Continuous Model to Real Model

The refractive-index distributions of these two piecewise continuous refractive index composites are given as

$$n(i, j) = [(i - 0.5)/NX]\Delta n_x + [(j - 0.5)/NY]\Delta n_y + n_0 \quad (i = 1, 2, 3, \ldots, NX;\ j = 1, 2, 3, \ldots, NY) \tag{11}$$

$$n(x, j) = (x/DX)\Delta n_x + [(j - 0.5)/NY]\Delta n_y + n_0 \quad (j = 1, 2, 3, \ldots, NY) \tag{12}$$

whereas the real medium has a spatially affine refractive-index distribution as

$$n(x, y) = (x/DX)\Delta n_x + (y/DY)\Delta n_y + n_0 \tag{13}$$

Thermal emission in the real medium is depicted by dashed lines in the following figures. The parameters selected for the calculation are $DX = 0.1$ m, $DY = 0.1$ m; $\Delta n_x = 0.6$, $\Delta n_y = 0.2$, $n_0 = 1.1$; and $\kappa = 10\ \mathrm{m}^{-1}$.

Only thermal emission whose polarization is perpendicular to the incident plane is discussed because the focus is on comparison of apparent emission in real and piecewise continuous media. Figure 3 shows the apparent thermal emission caused by the bar model. Figure 3a shows the emissivity distribution from a medium with refractive/reflective interfaces. Figure 3b presents the results for refractive/totally reflective interfaces. The reflectivity for perpendicular polarization at an interface is[20]

$$\rho_\perp(\zeta) = \left[\frac{\sin(\zeta - \theta)}{\sin(\zeta + \theta)}\right]^2 \tag{14}$$

Because of the assumption of an excessive number of interfaces in the bar model, which do not exist in the real medium, the difference between the two hypotheses could generate a much greater difference in the calculation of emissivity. As illustrated in Fig. 3a, the apparent emssivity from a GRIN medium employing a bar model defined by the refractive/reflective interface hypothesis differs greatly

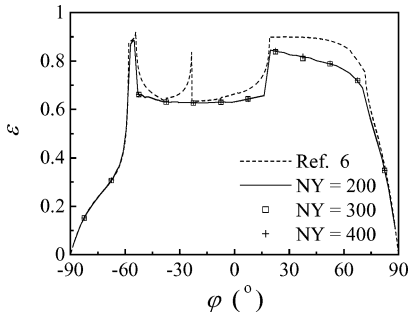

Fig. 3a Apparent perpendicular emissivity using the bar model with refractive/reflective interfaces ($x = 0.025$ m, $n_0 = 1.1$, $\Delta n_x = 0.6$, $\Delta n_y = 0.2$).

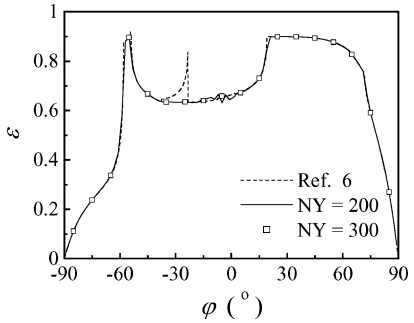

Fig. 3b Apparent perpendicular emissivity using the bar model with refractive/totally reflective interfaces ($x = 0.025$ m, $n_0 = 1.1$, $\Delta n_x = 0.6$, $\Delta n_y = 0.2$).

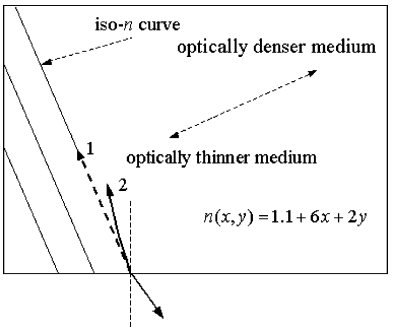

Fig. 4a Schematic diagram of trajectory whose tangent is parallel to iso-*n* curves.

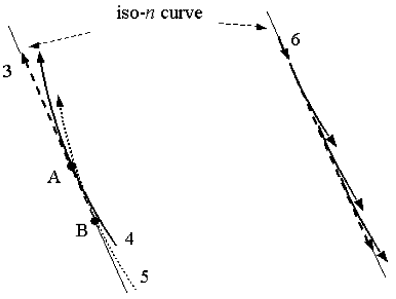

Fig. 4b Schematic diagram for a method of reductio ad absurdum.

from that from a medium with a spatially affine refractive-index distribution. Increasing the number of bars ($NX = NY + 1$ in calculation) does not reduce the difference and has no influence on the result when the number is large enough.

As illustrated in Fig. 3b, the apparent emissivity of a composite medium is similar to that of a medium with a spatially affine refractive-index distribution in most regions except for some directions, one of which is proximate to the normal direction. For the bar model, the radiation, which only goes along a straight line and is perpendicularly incident upon the Y plane, can go out of the medium normally. In a medium with a spatially affine refractive-index distribution, the ray's path is not a straight line, and only those rays whose tangents are normal to the surface can exit the medium perpendicularly. This causes a fluctuation of thermal emission along the normal direction of the composite medium, although this fluctuation is insignificant.

The significant difference at -23.28 deg, as shown in Fig. 3b, is mainly caused by the assumption of Ref. 6. At $x = 0.025$ m, the refractive angle in the medium corresponding to the emission angle of -23.28 deg is -18.43 deg, which is parallel to the iso-*n* curves. Refracted rays in this direction are assumed to be traveling in a straight line parallel to the iso-*n* curves as is described in Ref. 6, shown as line 1 in Fig. 4a. However, this assumption is incorrect. In a medium with a refractive-index distribution such as Eq. (13), only the trajectory perpendicular to the iso-*n* curves is straight. For other rays, whenever their tangents parallel the iso-*n* curves, total reflection occurs, and the ray will be guided to the side through a curved route, which is optically thicker, as represented by line 2 in Fig. 4a. This argument can be validated by a reductio ad absurdum proof. As shown in Fig. 4b, line 3 is a ray parallel to the iso-*n* curves. If ray 4 is tangent to line 3 at point A, it will merge into line 3 at this point, according to Ref. 6. If ray 5 is tangent to line 3 at point B, it will merge into line 3 as well. In this way, we can find many other rays that will follow this pattern. However, if we trace a ray along line 3 in the opposite direction such as line 6 in Fig. 4b, the ray will split into many different ones. This deduction is reasonable because propagation of light is reversible. However, such a split could not occur in the actual case. From the opinion of Ref. 6, we deduce a wrong conclusion. Therefore, the apparent emissivity around -23.28 deg given in Ref. 6 is incorrect. Nevertheless, for other emission angles the analysis in Ref. 6 is correct and has been confirmed by this paper.

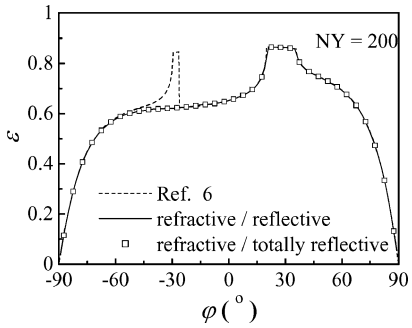

Fig. 5 Apparent perpendicular emissivity using the slab model ($x = 0.05$ m, $n_0 = 1.1$, $\Delta n_x = 0.6$, $\Delta n_y = 0.2$).

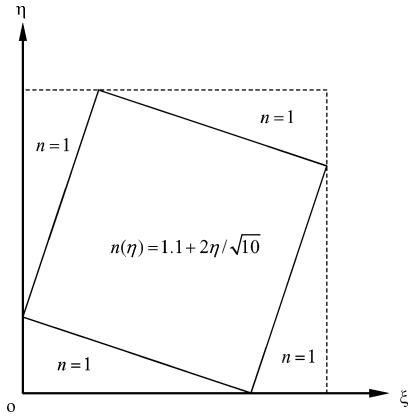

Fig. 6 New coordinate system for a GRIN semitransparent medium.

Figure 5 illustrates the apparent thermal emissivity using a slab model with different inner interface hypotheses. The influence of the inner interface hypothesis on radiative transfer and apparent thermal emission is relatively small because the slab model has inner interfaces to only one direction. The apparent emissivity of the slab model is the same as that of the bar model within the vicinity of the normal direction. It also matches the assumed thermal emissivity of a medium with a spatially affine refractive-index distribution in this region. Similar to the bar model, the calculation at -26.28 deg should also be corrected for the same reason already discussed.

Thermal emission in a semitransparent medium with a continuous refractive-index distribution was also calculated. The method used here is somewhat different from that used in Ref. 6. For a medium with a refractive-index distribution given by Eq. (13), a coordinate transformation is made as

$$x = (\xi - DY \sin\alpha)\cos\alpha + \eta \sin\alpha \tag{15}$$

$$y = -(\xi - DY \sin\alpha)\sin\alpha + \eta \cos\alpha \tag{16}$$

where $\alpha = \arctan[(\Delta n_x/DX)(DY/\Delta n_y)]$, which denotes the angle between the original coordinates and the transformed coordinates.

Figure 6 shows the current coordinates and the relative position of the semitransparent medium after the transformation. The refractive index distribution of $n(x, y) = 1.1 + 6x + 2y$ is changed to $n(\eta) = 1.1 + 2\eta/\sqrt{10}$, which is a one-dimensional linearly varying refractive index distribution. Thermal emission can be calculated by the curved ray tracing method in a one-dimensional GRIN semitransparent medium, as shown in Ref. 5. The ray tracing process is complex, so that only the results are shown here. Figure 7a shows the results of the apparent thermal emissivity of this GRIN medium, and Fig. 7b gives the relative errors between the results of the GRIN model and that of an approximate model with refractive/totally reflective inner interfaces. The relative error is defined as

$$\delta = \frac{\varepsilon_{\text{approximate model}} - \varepsilon_{\text{real model}}}{\varepsilon_{\text{real model}}} \times 100\% \tag{17}$$

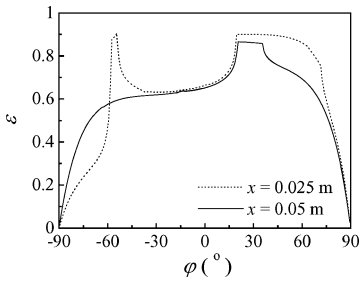

Fig. 7a Apparent perpendicular emissivity from a GRIN semitransparent medium, $n(x, y) = 1.1 + 6x + 2y$.

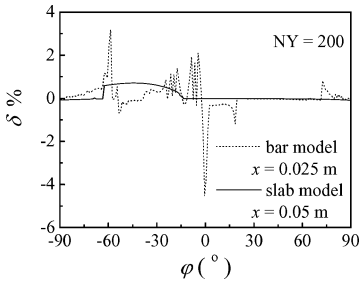

Fig. 7b Relative error of apparent perpendicular emissivity by approximate model, $n(x, y) = 1.1 + 6x + 2y$.

The results show that the absolute value of the relative error is less than 5% for the bar model, whereas for the slab model the absolute value of the relative error is less than 1%.

The preceding results and discussion show that Siegel and Spuckler's idea can be employed to solve multidimensional problems. The piecewise continuous refractive index model can be used to model semitransparent media with continuously variable refractive index distributions. The refractive/totally reflective inner interface hypothesis is an appropriate approach to model all forms of piecewise continuous refractive index media.

B. Thermal Emission in a GRIN Semitransparent Medium

In this section, we will calculate thermal emission from a semitransparent medium with a two-dimensional graded index using a slab model and the refractive/totally reflective inner interface hypothesis. Reflectivity at an interface is calculated according to Fresnel's law,[20]

$$\rho(\zeta) = \frac{1}{2}\left\{\left[\frac{\sin(\zeta - \theta)}{\sin(\zeta + \theta)}\right]^2 + \left[\frac{\tan(\zeta - \theta)}{\tan(\zeta + \theta)}\right]^2\right\} \tag{18}$$

The geometric parameters of the medium used in the calculations are $DX = 0.1$ m and $DY = 0.1$ m.

Figure 8 is the apparent directional emissivity of a semitransparent medium with a refractive index distribution defined as $n(x, y) = n_0 + a(x + y)$. Compared to the results using a constant refractive index ($a = 0$, Figs. 8d and 8e), the apparent emissivities of graded-index media ($a \neq 0$, Figs. 8a–8c, 8f, and 8g) show more complex anisotropy. A medium with constant refractive index has symmetrical apparent emission within the vicinity of the normal direction, whereas a medium with a spatially varying refractive index distribution shows an obviously asymmetric pattern. The variation in the apparent directional emissivity of a nonuniform refractive index medium is not smooth when its absorption coefficient is small ($\kappa = 4$ m^{-1}, Fig. 8a) and/or the variation of refractive index in the medium is large ($a = 9$, Fig. 8f). When the absorption coefficient is increased to $\kappa = 50$ m^{-1} (Fig. 8c), the influence of the refractive index distribution on the medium is weakened. In this case, the emissivity of a medium with a refractive-index distribution defined as $n(x, y) = 1.1 + 6(x + y)$ is similar to that of a constant refractive index because emissivity is mainly influenced by emission of the medium near the surface. When the variation in the refractive index

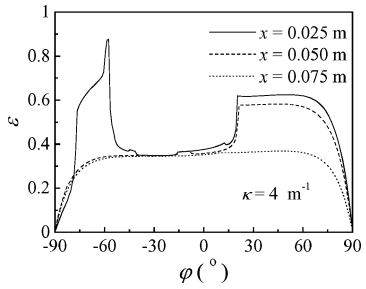

Fig. 8a Apparent emissivity of an isothermal medium, $n(x, y) = 1.1 + 6x + 6y$, $\kappa = 4\ \mathrm{m}^{-1}$.

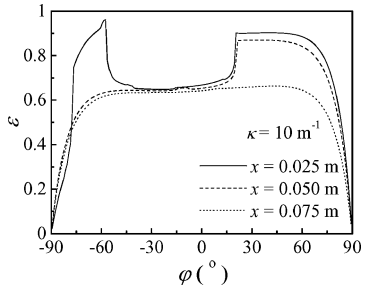

Fig. 8b Apparent emissivity of an isothermal medium, $n(x, y) = 1.1 + 6x + 6y$, $\kappa = 10\ \mathrm{m}^{-1}$.

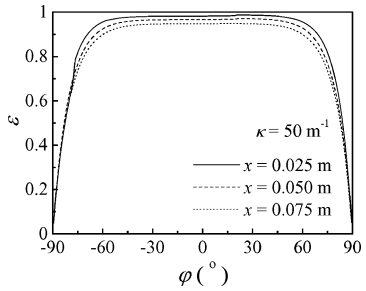

Fig. 8c Apparent emissivity of an isothermal medium, $n(x, y) = 1.1 + 6x + 6y$, $\kappa = 50\ \mathrm{m}^{-1}$.

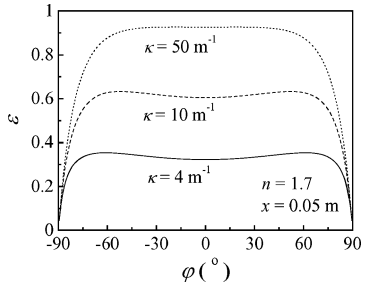

Fig. 8d Apparent emissivity of an isothermal medium, $n(x, y) = 1.7$.

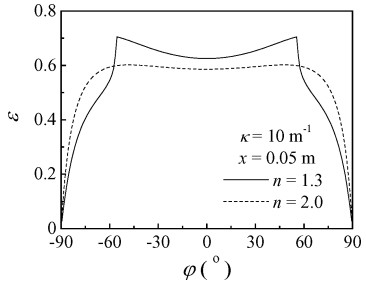

Fig. 8e Apparent emissivity of an isothermal medium, $n(x, y) = 1.3$ and $n(x, y) = 2.0$.

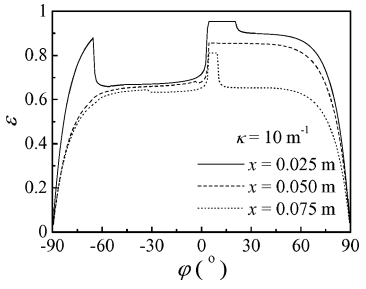

Fig. 8f Apparent emissivity of an isothermal medium, $n(x, y) = 1.1 + 9x + 9y$.

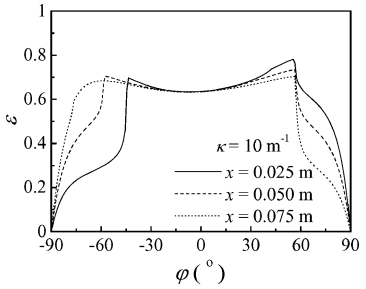

Fig. 8g Apparent emissivity of an isothermal medium, $n(x, y) = 1.1 + 2x + 2y$.

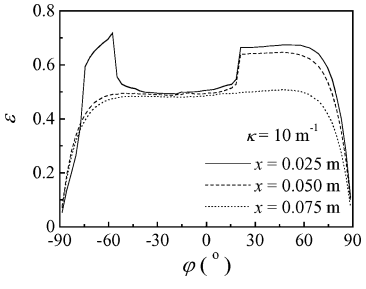

Fig. 9a Apparent emissivity of a nonisothermal medium, $n(x, y) = 1.1 + 6x + 6y$, $T = 500 + 3000y$.

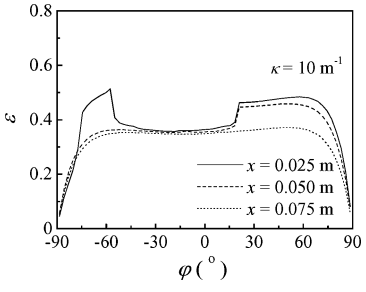

Fig. 9b Apparent emissivity of a nonisothermal medium, $n(x, y) = 1.1 + 6x + 6y$, $T = 800 - 3000y$.

of the medium is small ($a = 2$, Fig. 8g), its emissivity is similar to that of a medium with a constant refractive index, such as the results for $n = 1.3$.

The numerical method in this paper can be easily used to calculate the apparent emissivity of nonisothermal media and those media with other types of continuous refractive index distributions. Figures 9a and 9b illustrate the apparent emissivity of a medium with a refractive index distribution defined as $n(x, y) = 1.1 + 6x + 6y$. The temperature distributions in the medium are $T(y) = 500 + 3000y$ and $T(y) = 800 - 3000y$, respectively. Figures 10a and 10b show the calculated apparent emissivities resulting from refractive index distributions defined of $n(x, y) = 1.1 + 6x + 0.6\sin(10\pi y)$ and $n(x, y) = 1.7 + 6x - 0.6\sin(10\pi y)$, respectively. Compared to the emission from a medium with a refractive index distribution of

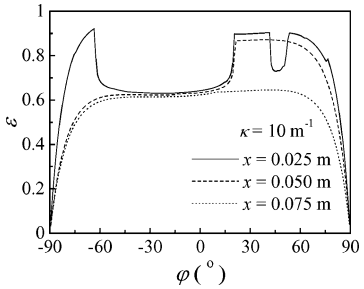

Fig. 10a Apparent emissivity of an isothermal medium, $n(x, y) = 1.1 + 6x + 0.6 \sin(10\pi y)$.

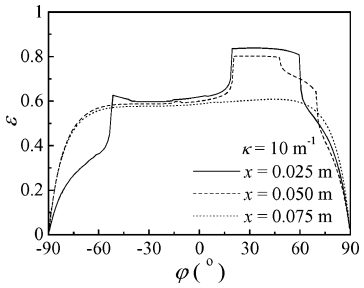

Fig. 10b Apparent emissivity of an isothermal medium, $n(x, y) = 1.7 + 6x - 0.6 \sin(10\pi y)$.

$n(x, y) = n_0 + a(x + y)$, the apparent emission is more irregular at some positions, such as 0.025 m in Fig. 10a and 0.05 m in Fig. 10b.

The bar model can be easily used for analysis of a medium with complex temperature fields and refractive index distributions (e.g., the refractive index is spatially nonlinear in two directions). Additionally, the numerical solution methods in this paper can be easily applied to solve three-dimensional problems.

IV. Conclusions

This study develops numerical solutions for the calculation of thermal emission in a two-dimensional semitransparent graded-index (GRIN) medium. Two types of piecewise continuous refractive-index composite models, the bar model and the slab model, are proposed to simulate a semitransparent GRIN medium. Also two types of interface hypotheses, the refraction/total reflection model and the reflection/refraction model, are discussed. Emissions in these two models based on different interface hypotheses are compared to the analytical results of Ref. 6.

The results of both models are generally satisfactory to approximate semitransparent GRIN media. At certain angles, there are significant differences between the emissivities obtained by the numerical methods we developed and those emissivities obtained by the analytical solutions in Ref. 6. Analysis shows that the differences in these directions are caused by an error in the ray trajectory along iso-n curves as described in Ref. 6.

The inner interface hypothesis influences the emissivity distribution of multidimensional problems. The numerical solutions of one-dimensional problems, which use the slab model to simulate a semitransparent medium with a continuously variable refractive index distribution and inner interface hypotheses, do not make any significant difference in the results.[17] The slab model was also applied to solve two-dimensional problems. However, the refractive/reflective inner interface hypothesis for the bar model generates notable errors in the calculation of emissivity. In reality, there are no inner interfaces in semitransparent media with continuously variable refractive index distributions, and there is no reflection except total reflection inside them. The inner interfaces change the ray trajectory. Thus the refractive/totally reflective inner interface hypothesis is better than the refractive/reflective inner interface hypothesis in depicting the reality of multidimensional problems if a bar model is adopted.

The simulations show that apparent emission is greatly influenced by the spatially varying refractive index. Thermal emission in a GRIN medium shows complex anisotropy and asymmetry, especially when the absorption coefficient is small and/or the refractive index varies greatly in the medium.

Acknowledgments

The project is supported by the China Postdoctoral Science Foundation (No. 2003.03). The authors appreciate the help of Ben Abdallah.

References

[1]Siegel, R., and Spuckler, C. M., "Variable Refractive Index Effects on Radiation in Semitransparent Scattering Multilayered Regions," *Journal of Thermophysics and Heat Transfer*, Vol. 7, No. 4, 1993, pp. 624–630.

[2]Siegel, R., "Refractive Index Effects on Local Radiative Emission from a Rectangular Semi-Transparent Solid," *Journal of Thermophysics and Heat Transfer*, Vol. 8, No. 3, 1994, pp. 625–628.

[3]Tan, H. P., Wang, P. Y., and Xia, X. L., "Transient Coupled Radiation and Conduction in an Absorbing and Scattering Composite Layer," *Journal of Thermophysics and Heat Transfer*, Vol. 14, No. 1, 2000, pp. 77–87.

[4]Liou, B. T., and Wu, C. Y., "Radiative Transfer in a Multi-Layer Medium with Fresnel Interfaces," *Heat and Mass Transfer*, Vol. 32, No. 1–2, 1996, pp. 103–107.

[5]Ben Abdallah, P., and Le Dez, V., "Thermal Emission of a Semi-Transparent Slab with Variable Spatial Refractive Index," *Journal of Quantitative Spectroscopy and Radiative Transfer*, Vol. 67, No. 3, 2000, pp. 185–198.

[6]Ben Abdallah, P., and Le Dez, V., "Thermal Emission of a Two-Dimensional Rectangular Cavity with Spatial Affine Refractive Index," *Journal of Quantitative Spectroscopy and Radiative Transfer*, Vol. 66, No. 6, 2000, pp. 555–569.

[7]Huang, Y., Xia, X. L., and Tan, H. P., "Coupled Radiation and Conduction in a Graded Index Layer with Specular Surfaces," *Journal of Thermophysics and Heat Transfer*, Vol. 18, No. 2, 2004, pp. 281–285.

[8]Liu, L. H., "Discrete Curved Ray-Tracing Method for Radiative Transfer in an Absorbing-Emitting Semitransparent Slab with Variable Spatial Refractive Index," *Journal of Quantitative Spectroscopy and Radiative Transfer*, Vol. 83, No. 2, 2004, pp. 223–228.

[9]Xia, X. L., Huang, Y., and Tan, H. P., "Thermal Emission and Volumetric Absorption of a Graded Index Semitransparent Medium Layer," *Journal of Quantitative Spectroscopy and Radiative Transfer*, Vol. 74, No. 2, 2002, pp. 235–248.

[10]Huang, Y., Xia, X. L., and Tan, H. P., "Comparison of Two Methods for Solving Radiative Heat Transfer in a Gradient Index Semitransparent Slab," *Numerical Heat Transfer, Part B*, Vol. 44, No. 1, 2003, pp. 83–99.

[11]She, H., and Tan, S., "Development and Application Prospects of High-Energy Laser Weapon," *Infrared and Laser Engineering*, Vol. 31, No. 3, 2002, pp. 267–271.

[12]Zhao, L., "Thermal Optical Evaluation to Optical Windows of Space Camera," *Acta Optica Sinica*, Vol. 18, No. 10, 1998, pp. 1440–1444.

[13]Zhao, L., and Shao, Y., "Summary of Thermal Control and Thermal Optical Analysis for Space Optical System," *Spacecraft Recovery and Remote Sensing*, Vol. 22, No. 2, 2001, pp. 13–19.

[14]Qiao, Y. T., *Graded Index Optics*, Science Press, Beijing, 1991, pp. 1–35.

[15]Adsten, M., Joerger, R., Jarrendahl, K., and Wackelgard, E., "Optical Characterization of Industrially Sputtered Nickel-Nickel Oxide Solar Selective Surface," *Solar Energy*, Vol. 68, No. 4, 2000, pp. 325–328.

[16]Tesfamichael, T., and Wackelgard, E., "Angular Solar Absorptance and Incident Angle Modifier of Selective Absorbers for Solar Thermal Collectors," *Solar Energy*, Vol. 68, No. 4, 2000, pp. 335–341.

[17]Huang, Y., Liang, X. G., and Xia, X. L., "Monte Carlo Simulation of Radiative Transfer in Scattering, Emitting, Absorbing Slab with Gradient Index," *Journal of Quantitative Spectroscopy and Radiative Transfer*, Vol. 92, No. 1, 2005, pp. 111–120.

[18]Ben Abdallah, P., Charette, A., and Le Dez, V., "Influence of a Spatial Variation of the Thermo-Optical Constants on the Radiative Transfer Inside an Absorbing-Emitting Semi-Transparent Sphere," *Journal of Quantitative Spectroscopy and Radiative Transfer*, Vol. 70, No. 3, 2001, pp. 341–365.

[19]Modest, M. F., "Backward Monte Carlo Simulations in Radiative Heat Transfer," *Journal of Heat Transfer*, Vol. 125, No. 1, 2003, pp. 57–62.

[20]Siegel, R., and Howell, J. R., *Thermal Radiation Heat Transfer*, 4th ed., Taylor and Francis, New York and London, 2002, pp. 71–106.